Liver Cyst Cytokines Promote Endothelial Cell Proliferation and Development

KELLEY S. BRODSKY, RYAN R. MCWILLIAMS, CLAUDIA R. AMURA, NICHOLAS P. BARRY, AND R. BRIAN DOCTOR[1]

University of Colorado Health Sciences Center, Department of Medicine, Denver, Colorado 80045

Autosomal dominant polycystic kidney (ADPKD) is highly prevalent genetic disease. Liver cyst disease is the most common extrarenal manifestation in ADPKD and accounts for up to 10% of ADPKD morbidity and mortality. The clinical features of ADPKD liver disease arise from dramatic increases in liver cyst volumes. To identify mechanisms that promote liver cyst growth, the present study characterized the degree of vascularization of liver cyst walls and determined that cyst-specific cytokines and growth factors can drive endothelial cell proliferation and development. Microscopic techniques demonstrated liver cyst walls are well vascularized. A comparative analysis found the vascular density in free liver cyst walls was greater in mice than in humans. Treatment of human microvascular endothelial cells (HMEC-1) with human liver cyst fluid (huLCF) induced a rapid increase in vascular endothelium growth factor receptor 2 (VEGFR2) phosphorylation that persisted for 45–60 min and was blocked by 20 μM SU5416, a VEGFR tyrosine kinase inhibitor. Similarly, huLCF treatment of HMEC-1 cells induced an increase in the cell proliferation rate (131 ± 6% of control levels; $P > 0.05$) and the degree of vascular development ('tube' diameter assay: 92 ± 14 μm for huLCF vs. 12 ± 7 μm for vehicle); $P > 0.05$). Both cell proliferation and vascular development were sensitive to SU5416. These studies indicate that factors secreted by liver cyst epithelia can activate VEGF signaling pathways and induce endothelial cell proliferation and differentiation. The present studies suggest that targeting VEGFR2-dependent angiogenesis may be an effective therapeutic strategy in blocking ADPKD liver cyst vascularization and growth. Exp Biol Med 234:1155–1165, 2009

Key words: vascular endothelial growth factor, VEGFR2, interleukin-8, CXCR2, angiogenesis

Introduction

Autosomal polycystic kidney disease (ADPKD) is a genetic disease that affects ~1 in 800 individuals. ADPKD is most noted for the development of grossly cystic kidneys and the subsequent loss of renal function. ADPKD accounts for ~5% of all cases of end-stage renal disease. Liver cysts are present within 94% of all ADPKD subjects over 35 years of age (1), and liver cyst disease accounts for up to 10% of ADPKD morbidity and mortality. The enormous increases in liver volumes, which can reach up to seven times normal (2), result in compression of surrounding organs, tissues and vessels and are responsible for the clinical manifestations of ADPKD (3). To reduce liver cyst volumes, current treatments are largely surgical, ranging from laproscopic fenestration of superficial liver cysts to liver transplantation. Significant efforts are currently underway to develop mechanism-based medical therapies that would intercede in the molecular and cellular pathways that drive liver cyst growth.

The clinical presentation of ADPKD is markedly heterogeneous, and both genetic and supragenetic pathways contribute to liver cyst growth. Mutations in the genes for either polycystin-1 or polycystin-2 are definitively linked with cystogenesis. As a molecular recessive disease, the timing, type and gene position of the second, somatic mutation likely has a significant impact on the onset, development and severity of the disease. More recently, modifier genes and supragenetic pathways have also emerged as pivotal contributors to the progression of cyst growth (4, 5). Among these supragenetic pathways, cyst-lining epithelial cells release specific cytokines and growth factors into the cyst fluids, where they can initiate autocrine/paracrine signaling of cell proliferation. Interestingly, renal and liver cysts secrete disparate profiles of cytokines and growth factors (6–8). In human liver cyst fluids (huLCF), vascular endothelium growth factor A (VEGF-A) and interleukin-8 (IL-8) are consistently elevated to levels above the K_m for their receptors (6, 9, 10). Likewise, in pkd2(WS25/-) mice, a genetic mouse model of human ADPKD (11), VEGF-A and KC, a murine analog of human IL-8, are similarly elevated (7, 8). The potential role these

This work was supported by the PKD Foundation (109a2r: RBD) and the University of Colorado Chancellor's Bridge Grant (RBD)

[1] To whom correspondence should be addressed at University of Colorado, Denver, Box B146, Room 10121, 12700 E. 19th Avenue, Aurora, CO 80045. E-mail: brian.doctor@ucdenver.edu

Received March 18, 2009.
Accepted May 26, 2009.

DOI: 10.3181/0903-RM-112
1535-3702/09/23410-1155$15.00

factors may play in dictating liver cyst growth was shown in pkd2(WS25/-) mice treated with SU5416, an inhibitor of VEGF tyrosine kinase activity (7). At 12 months of age (8 months of treatment), liver weights in vehicle-treated pkd2(WS25/-) mice were three times normal weight, while livers in SU5416-treated mice were not grossly cystic and had no significant increase in weight.

The potential cellular site(s) that account for this profound effect include the cyst-lining epithelium and vascular endothelial cells within the liver cyst wall. Liver cyst-lining epithelial cells express receptors for VEGF-A and IL-8 (KC) (6, 12), and treatment of liver cyst epithelial cells with VEGF-A, KC or mouse liver cyst fluid induces a robust proliferative response (7, 8, 12). These implicate the liver cyst-wall epithelial cells in responding to VEGF-A and IL-8 (KC) and promoting liver growth. VEGF-A and IL-8 are also potent pro-angiogenic factors, and studies suggest VEGF-A and IL-8 (KC) are secreted across the basolateral membrane of liver cyst epithelial cells, where they could interact with the vascular endothelium. Given the potential role the vasculature could play in the growth and maintenance of ADPKD liver cysts, the present study seeks to characterize the vasculature within liver cyst walls and to determine the capacity of factors released by liver cyst-lining epithelial cells to drive endothelial cell proliferation and vascular development.

Materials and Methods

Reagents. Unless otherwise noted, all cell culture media and reagents were purchased from Gibco-Invitrogen (Grand Island, NY). Fetal Bovine Serum (FBS) was purchased from Hyclone-QB Perbio (Logan, UT). Growth factor-reduced Matrigel was purchased from BD Biosciences (San Jose, CA). All tissue culture plastic materials were purchased from Beckton Dickinson (Lincoln Park, NJ). VEGF-A and IL-8 were purchased from R&D Systems (Minneapolis, MN). Commercial antibodies used included those against vascular endothelium growth factor receptor 2 (VEGFR2; ABR-ThermoFisher; Rockford, IL), Tyr951-phosphorylated VEGFR2 (Santa Cruz; Santa Cruz, CA), von Willebrand Factor antibody (Sigma Immunochemicals; St. Louis, MO) and actin (Calbiochem; San Diego, CA). Rhodamine-labeled goat anti-rabbit secondary antibody was obtained from Jackson ImmunoLaboratories (West Grove, PA). 4′,6-diamidino-2-phenylindole (DAPI) was obtained from Molecular Probes (Eugene, OR). Protease inhibitors (Complete protease inhibitor cocktail) were obtained from Roche (Indianapolis, IN). Phosphatase inhibitors (Phosphatase Inhibitor Cocktail II) were obtained from Calbiochem (LaJolla, CA). HRP-tagged secondary antibodies and SuperSignal luminol were obtained from Pierce (Rockford, IL). SU5416 was provided by Dr. Norbert Voelkel (Virginia Commonwealth University).

Human ADPKD Liver Cyst Fluid Samples. The collection of liver cyst fluids and liver cyst wall tissue from human patients was done in accordance with a protocol reviewed and approved by the Colorado Multiple Institution Review Board. All patients were fully informed and consented to participate in these studies. Fluids from liver cysts were obtained during laparoscopic fenestration procedures by needle aspiration. All cyst fluid samples were immediately frozen in liquid nitrogen and stored at −80°C until needed. All human cyst fluid samples had VEGF-A and IL-8 levels that exceeded the Km for their respective receptors. Liver cyst wall tissue was obtained surgically by 'deroofing' large, accessible liver cyst walls that had grown out from the body of the liver. These tissues were immediately placed in fixative (1% glutaraldehyde, 2% paraformaldehyde and 50 mM cacodylate; pH 8.0; room temp) and stored at 4°C until further processing. Removal of information that would permit identification of the donors disallows the demographic data on the liver cyst fluids to be compared and contrasted.

Pkd2(WS25/-) Mouse Model. C57BL/6 *pkd2*(WS25/-) mice were developed by Stefan Somlo (Yale University), who provided *pkd2*(+/-) and *pkd2*(WS25/+) breeding pairs for this project. Mice were genotyped by Southern blotting as previously reported (11). *Pkd2*(WS25/-) mice closely model the molecular recessive characteristics of the human condition by having one copy of *pkd2* knocked out and having a second, recombinant-sensitive allele (*i.e.*, WS25) that undergoes high rates of recombination to yield knock outs of the second copy of the gene in somatic cells during the life span of the animals. By four months of age, all *pkd2*(WS25/-) mice develop discernible kidney and liver cysts (11). Over the ensuing months, liver cysts grow out from the body of the liver.

***In Situ* Imaging of Blood Vessels in Mouse Liver Cyst Walls.** *In situ* light microscopy was used to assess the presence of blood vessels in an intact mouse liver cyst wall. Multiple cysts were evaluated in two separate mice. Briefly, pkd(WS25/-) mice were raised for 8+ months to allow large liver cysts to grow away from the liver. Mice were euthanized by intraperitoneal pentobarbital (60 mg/kg body weight), the abdominal cavity was opened, and the mice were positioned on their sides within an imaging chamber fitted with a glass slide in the chamber floor. The liver cysts were positioned to allow the direct passage of light from the condenser, through the liver cysts and into the ×10 objective lens. The images were captured by color digital camera on an inverted microscope (Zeiss Axiovert100 microscope with axiocam HRc and axiovision digital image acquisition software).

Immunohistologic Imaging of the Vasculature in Mouse Liver Cyst Walls. Immunofluorescence microscopy was used to confirm the presence of endothelial cells within the putative vascular structures and to evaluate the positioning of blood vessels within mouse liver cyst walls (6). Cyst walls from three mice were evaluated. Briefly, liver cyst walls that had grown away from the liver were excised and placed in 3% paraformaldehyde in phosphate-buffered saline (pH 7.4). The tissue was then

embedded in OCT, frozen in liquid nitrogen, and cryosectioned (10 μm). Tissue sections were blocked (60 min; 10% normal goat serum and 0.1% Tween 20 in phosphate buffered saline (PBS), washed (0.1% Tween 20 in PBS), incubated with an anti-von Willebrand Factor antibody (60 min; 1:100), washed, incubated in rhodamine-labeled goat anti-rabbit secondary antibody (1:100) containing DAPI (1:1,000), washed, and mounted in mowiol. Sections were imaged by standard confocal microscopy (Zeiss 510 LSM; UCHSC Light Microscopy Core Facility).

Second Harmonic Generation Imaging of Mouse Liver Cyst Walls. The spatial relationship of the cyst-lining epithelium and vascular endothelium within mouse liver cyst walls was evaluated *in situ* by pre-labeling nuclei *in vivo* and detecting autofluorescence from the pervasive, fibrous extracellular matrix proteins that reside within the liver cyst wall using second harmonic generation (SHG) fluorescence imaging (13). Fifteen minutes prior to the start of the study, pkd2(WS25/-) mice (8 to 12 months of age) received Hoechst 33342 (IP; 250 mg in saline) to fluorescently label nuclei *in vivo*. The mice were then euthanized by intraperitoneal pentobarbital (60 mg/kg body weight), the abdominal cavity was opened, the mice were positioned on their sides, and large superficial cysts were positioned to rest atop a glass coverslip in the chamber floor. Imaging was carried out using a Zeiss 510 NLO META inverted confocal microscope equipped with a femtosecond pulsed Ti Sapphire laser (Chameleon Ultra; Coherent, Santa Clara). The liver cyst was imaged using a ×40/1.2NA objective. The laser was tuned to 800 nm and simultaneously generated an SHG signal from collagen fibers and two photon excitation fluorescence from the Hoechst 33342 dye. The emitted signal was first passed through a BG39 filter to remove residual excitation laser light. The two signals were separated in the Zeiss META spectral detector with user defined filter ranges of 380 nm to 400 nm for the SHG signal and 420 nm to 460 nm for the Hoechst 33342 signal. Image stacks were collected and processed in the Zeiss 510 control software.

Electron Microscopic Morphometry of Liver Cyst Walls. Electron microscopy was used to measure the vascular density and vessel-to-epithelium distances within human and mouse liver cyst walls (6, 14). Liver cyst wall tissues were fixed (1% glutaraldehyde, 2% paraformaldehyde and 50 mM cacodylate; pH 8.0; ≥60 min), post-fixed in 1% osmium, dehydrated in ethanol, embedded in Epon-812, and stained with uranyl acetate and lead citrate. Tissue sections were examined by transmission electron microscopy (UCHSC Electron Microscopy Core Facility). Area measurements of the epithelium and vascular spaces in mouse and human liver cyst walls were made on scanned images of electron micrographs using NIH Image, as previously described (14). Liver cyst walls from four human subjects and four distinct mice were evaluated.

HMEC-1 Cell Culture. Human HMEC-1 cells (15) were cultured in MCDB-131 supplemented with 10% FBS, 2.5 mM L-glutamine, 10 ng/ml epidermal growth factor (Upstate Biotechnology; Lake Placid, NY) and 1 μg/ml hydrocortisone (Sigma; St. Louis, MO). Cells were harvested with 0.25% trypsin-EDTA and passaged once a week. Cells were maintained at 37°C under a humidified atmosphere with 5% CO_2. Worthy of note, these cells are a well-established human microvascular endothelial cell line that displays consistent phenotypic responses to VEGF and IL-8. These responses are paralleled by the responses measured in hMVEC cells, another human microvascular endothelial cell line.

Western Blotting. Western blotting for total and Tyr-951-phosphorylated VEGFR2 was performed as previously described (16). Briefly, cells were lysed in ×5PAGE (5% SDS, 25% sucrose, 5 mM EDTA, 50 mM Tris-HCl and 5% 2-mercaptoethanol; pH 8.0; protease inhibitors; phosphatase inhibitors). Proteins within these lysates were separated by electrophoresis through a 4–14% gradient gel (50V for 30 min; 200V for 3 hr) and transferred onto nitrocellulose (300 mA for 3.5 hr). These blots were blocked with 5% non-fat dry milk, incubated with primary antibody solutions (60 min), washed, incubated with HRP-tagged secondary antibody solutions (1:10,000 dilution, 30 min), washed, and incubated in SuperSignal Luminol (1 min); emitted light was imaged on a UVP Photodocumentation System.

Cell Proliferation Assay. The proliferation rates of the HMEC-1 cells were measured by Alamar Blue assay, as described by the manufacturer (Biosource/Invitrogen; Carlsbad, CA). Foundational dose-response studies were first performed to identify the minimal concentration of VEGF-A and IL-8 that consistently elicited a response. Briefly, cells were seeded at sub-confluent density into 6-well plates, allowed to attach overnight in supplemented media, and then incubated for 24 hr in serum-free media. Cells maintained in serum-free media served as a baseline control; media containing 10% FBS served as a positive control. In experimental groups, cells grown in serum-free media were treated with 10 ng/ml VEGF-A, 10 ng /ml IL-8 or 10% huLCF with or without 20 μM SU5416. Subsequently, serum-free media containing 10% Alamar Blue was added to the cells for 2 hr, the media was evaluated for absorbance at 540 nm and 600 nm, and the reduction of Alamar Blue calculated as directed by the manufacturer. The effects of twelve separate huLCF samples were measured.

HMEC-1 Cell 'Tube' Formation Assay. The ability of VEGF-A, IL-8 and huLCF to affect the vascular modeling capacity of HMEC-1 cells was measured using a 'tube' formation assay (17, 18). Cold growth factor-depleted Matrigel (250 μl) was added to the wells of a 24-well plate and transferred to a cell culture incubator (37°C; 5% CO_2) for 30 min. HMEC-1 cells were resuspended in MCDB-131 media (100,000 cells/ml), and 0.5 ml of cell suspension was added to each well. Factors to be tested (10 ng/ml VEGF-A, 10 ng/ml IL-8 and 10% human liver cyst fluid) and VEGFR

tyrosine kinase inhibitor (20 μM SU5416) were added to the appropriate media prior to resuspending the cells. Cells were allowed to seed and develop for 24 hr prior to imaging for 'tube' formation. Initial studies confirmed that similar numbers of cells seeded on the matrix independent of the additives. Images were obtained using phase contrast microscopy (Nikon; ×40 objective) and captured by a digital camera (Spot Camera; Diagnostic Instruments). 'Tube' diameters were calculated from four distinct preparations. Within each preparation, four to six random fields were selected and the diameter of each 'tube' in the field measured in the mid-region of the 'tube.'

Statistical Analysis. All statistics were evaluated by GraphPad Instat (San Diego, CA) analysis software. The statistical analysis first compared the values of individual groups using a Mann-Whitney non-parametric analysis. Groups were considered significantly different at $P < 0.05$. Subsequently, the means of multiple groups in each quantitative study were subjected to an analysis of variance. A Tukey multiple comparisons test was performed to identify which groups were significantly different ($P < 0.05$). The results from these two statistical approaches were the same. The results from the analysis of variance were presented in Figures 5 and 7. Groups without a shared letter were significantly different from each other.

Results

Mouse Liver Cyst Walls Are Well-Vascularized. Three light microscopy techniques were used to qualitatively assess the vascularization of liver cyst walls in pkd2(WS25/-) mice. Providing a broad perspective, *in situ* light microscopy imaging through intact mouse liver cysts revealed an abundance of branched vessels of differing diameters throughout the liver cyst walls (Fig. 1A). Fixation of these walls and subsequent immunostaining and fluorescence imaging of von Willebrand Factor, an endothelial cell marker, confirmed the observed structures were endothelial cell-lined blood vessels. Numerous small diameter vessels were readily found within 20–30 μm of the epithelial cell layer that lines the lumen of the cysts (Fig. 1B). Second harmonic generation-confocal microscopy was then used for *in situ* optical sectioning of mouse liver cyst walls to evaluate the relative positioning of vascular structures to the fibrous proteins that comprise the mass of the liver cyst wall (Fig. 2). These studies demonstrated that vascular structures were embedded in the middle of the fibrous protein-rich liver cyst wall. The relatively close apposition of many of these vessels to the cyst-lining epithelial cell layer would be expected to allow efficient gas and nutrient exchange.

Vascular Features in Human Versus Mouse Liver Cysts. Electron microscopy was used to provide a quantitative characterization of liver cyst walls from both mice and humans. As shown previously (6) and consistent with the fibrous proteins observed in Figure 2, the majority

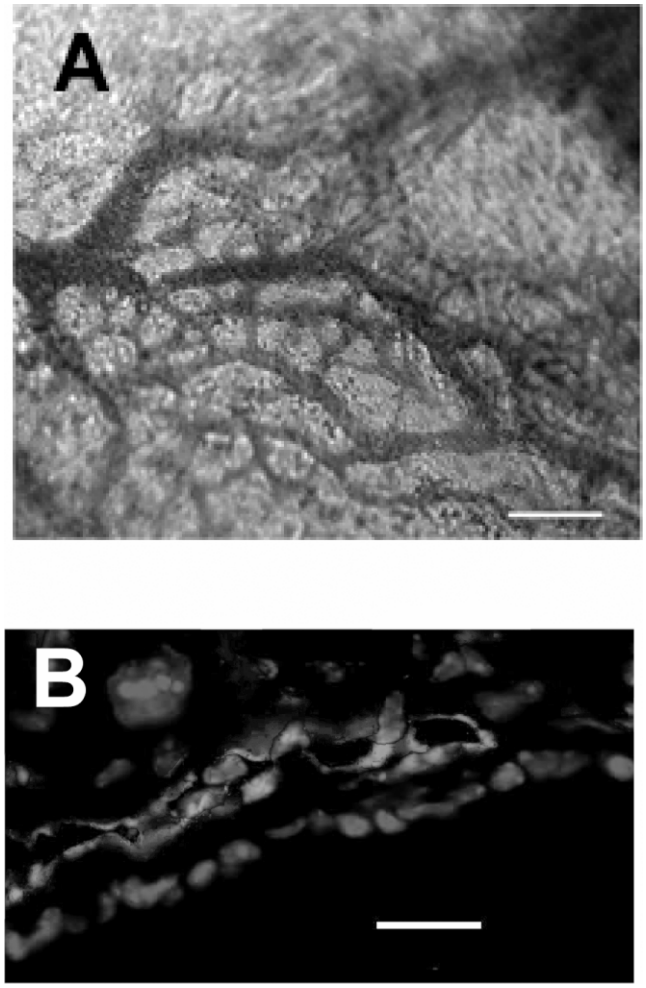

Figure 1. Liver cyst walls are vascularized. (A) Transmission light imaging through pkd2(WS25/-) mouse liver cysts reveals an abundance of blood vessels throughout the cyst walls (bar = 100 μm). (B) Fluorescence imaging of endothelial cells (red = von Willebrand factor) shows the presence and relative position of the endothelial cells within liver cyst walls. Staining of nuclei within the liver cyst wall (blue = DAPI) shows the presence of putative fibroblasts within the cyst wall and the epithelial layer that lines the interface of the cyst wall and lumen (bar = 50 μm; positioned in the cyst lumen). A color version of this figure is available in the online journal.

of the cyst wall is comprised of fibrous extracellular matrix proteins. Interestingly, the vascular densities and vessel-to-epithelium distances in human and mouse liver cyst walls were significantly different. In liver cyst walls from pkd2(WS25/-) mice, 7.4 ± 2.6% of the cyst wall volume was occupied by the vasculature (Fig. 3A). In contrast, only 1.0 ± 0.9% of the cyst wall volume in human liver cyst walls was occupied by vascular spaces. In addition, the vasculature that is present within human liver cyst walls resides at greater distances from the epithelium-lined lumenal surface (Fig. 3B). In pkd2(WS5/-) mice, the vessels reside, on average, 25 ± 3 μm from the epithelial layer. In humans, the vessels reside 91 ± 35 μm from the epithelial layer. The presence of much more extracellular matrix

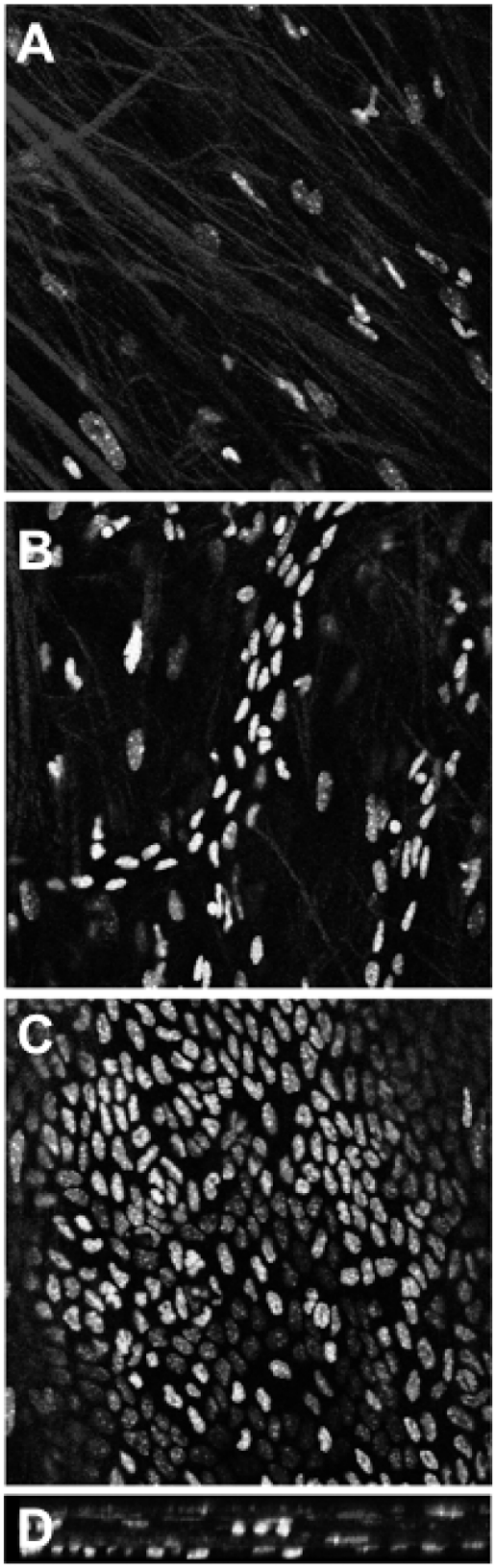

Figure 2. In situ imaging of liver cyst wall topography. The three dimensional organization of the connective tissue, vasculature and epithelial cells within pkd2(WS25/-) mouse liver cyst walls was imaged *in situ* by serial optical sectioning using confocal microscopy. Shown are Hoechst 33342-stained nuclei (green) and Second Harmonics Generated fibrous proteins (blue) from a representative liver cyst wall (~30 μm thick) that had grown out from the body of the liver. (A) The outer regions of the liver cyst walls (distance = 8 μm from outer surface) were comprised mainly of fibrous proteins (blue). Observed nuclei (green) were likely from fibroblasts. (B) In the middle of the cyst wall (distance = 17 μm from outer surface), well-defined, putative vascular structures lined by endothelial cells were found within this region. (C) Epithelial cells line the lumenal surface (distance = 26 μm from the outer surface) of the liver. (D) An XZ-section image of the liver cyst wall (top of panel: exterior surface; bottom of panel: lumenal surface) highlights the presence of nuclei from vascular structures positioned in the middle of the cyst wall and epithelial cell nuclei lining the lumenal surface. A color version of this figure is available in the online journal.

material within the human liver cyst wall likely accounts for disparity. This is highlighted by the differences in the density of the epithelial cell layer. While the size of individual human and mouse liver cyst-lining epithelial cells are similar, the epithelial layer comprises 14.6 ± 1.5% of the cyst wall volume in mice and only 2.4 ± 1.1% in humans.

Liver Cyst Fluid Induces Phosphorylation of VEGFR2. Specific cytokines and growth factors are released across the apical membrane of cyst-lining epithelial cells and accumulate in liver cyst fluids (6–8). The same pattern of release is observed across the basolateral membrane (8). VEGFR2 and CXCR2 ligands are consistently released from these epithelial cells and work cooperatively to activate the VEGFR2 signaling pathway (19). Consequently, huLCF was used to approximate the basally released factors, and the capacity of media containing 10% huLCF to induce VEGFR2 phosphorylation in HMEC-1 cells was evaluated. All huLCF samples contained concentrations of VEGF-A and IL-8 above the Km for their respective receptors (data not shown) 6, 7). As previously published (19), both VEGF-A and IL-8 promoted a rapid increase in VEGFR2 phosphorylation (data not shown). The late segment of the previously reported biphasic response was not observed in the present studies, but the robust early response was consistently observed. Both the VEGF-A-dependent and IL-8-dependent increase in VEGFR2 phosphorylation was markedly inhibited by pre-treatment with 20 μM SU5416, a VEGFR tyrosine kinase inhibitor (20). Treatment of HMEC-1 cells with 10% huLCF similarly induced a rapid increase in Tyr951 phosphorylation of VEGFR2 (Fig. 4A). The elevated phosphorylation levels peaked around 10 min, persisted for 45–60 min, and returned to basal levels after 90 min. Pre-treatment of the HMEC-1 cells with 20 μM SU5416 markedly inhibited the huLCF-induced increase in VEGFR2 phosphorylation. (Fig. 4B). The results shown are representative of two full time course studies without and with SU5416 pre-treatment.

Liver Cyst Fluid Induces Endothelial Cell Proliferation. To gain insight into this angiogenic potential, the capacity of huLCF to drive HMEC-1 proliferation was

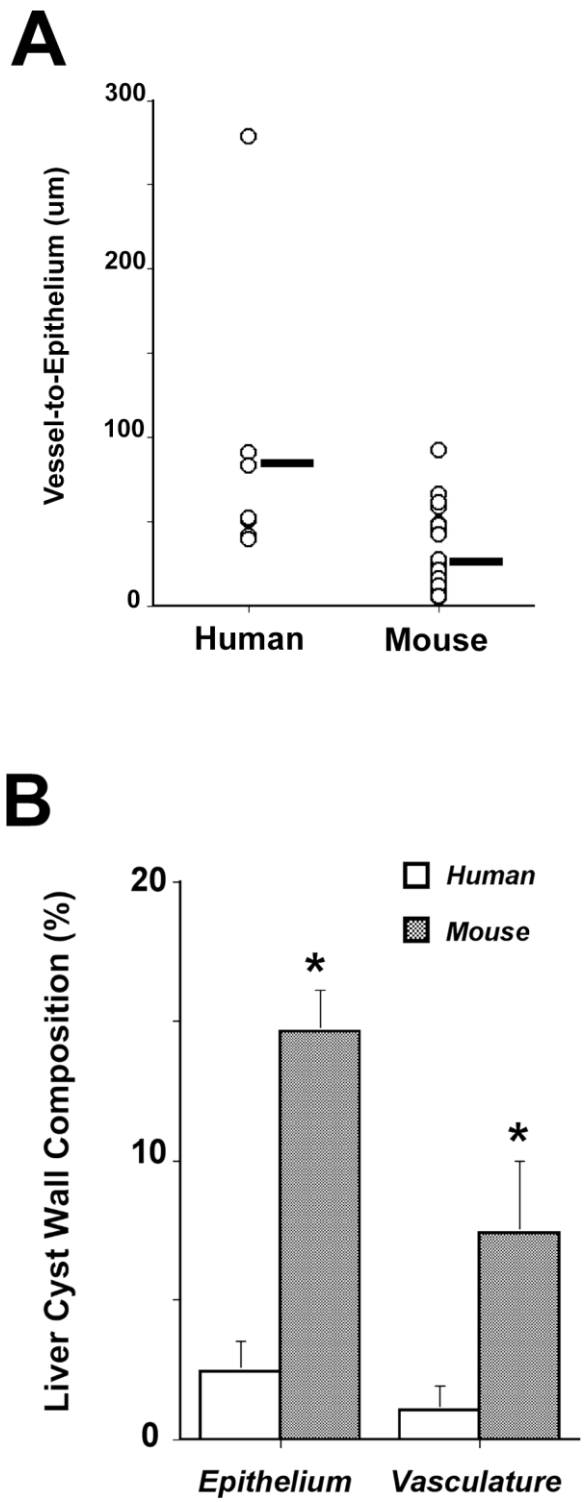

Figure 3. Comparative vascularization of human and mouse liver cyst walls. Morphometric analyses of vessel-to-epithelium distances, epithelial densities and vascular densities were performed on liver cyst walls that had grown out from the body of human and mouse livers. (A) Distances from the blood vessels to the epithelial layers were significantly greater in human liver cyst walls (91 ± 35 μm; n = 7) than in mouse liver cyst walls (25 ± 3 μm; n = 37). (B) The percentage of the liver cyst wall comprised of epithelial cells was less in human (2.4 ± 1.1% of total liver cyst wall volume; n = 4) than in mice (14.6 ± 1.5% of total liver cyst wall volume; n = 4). Similarly, blood vessel volumes in human liver cyst walls (1.0 ± 0.9% of total liver cyst wall volume; n = 4) were markedly lower than volumes measured in mouse liver cyst walls (7.4 ± 2.6% of total liver cyst wall volume; n = 4).

evaluated. Incubation of HMEC-1 cells with 10% huLCF induced a significant proliferative response (131 ± 6; n = 12) compared to cells in unsupplemented media (100 ± 0; n = 3) and in 10% FBS (Serum: 153 ± 11; n = 3). Pretreatment with 20 μM SU5416 had no discernible effect on the proliferative rates in unsupplemented cells (103 ± 2; n = 3) or cells incubated with 10% FBS (149 ± 9; n = 3). This indicates the basal rates of proliferation and the serum-induced proliferation do not require active VEGF signaling. In contrast, SU5416 markedly inhibited the proliferative response to 10% huLCF (80 ± 6; n = 12), indicating that VEGFR signaling has a pivotal role in transducing the proliferative response to the factors present in huLCF.

Liver Cyst Fluid Induces Endothelial Development. To get a broader sense of the capacity of huLCF to drive angiogenesis, a 'tube formation' assay was employed (17, 18). In this assay, HMEC-1 cells were seeded in GF-reduced matrigel and exposed to potential stimuli, and the multi-cellular morphology followed for 24 hr. Preliminary studies found that 'activated' HMEC-1 cells rapidly migrate together to form cell clusters. These clusters sprout cellular extensions (or 'tubes') that join with sprouts from neighboring clusters. These 'tubes' increase in diameter and complexity over time. In a comparative series of studies taken at 24 hr after seeding (Fig. 6), unsupplemented HMEC-1 cells showed evidence of some migration and the beginnings of 'tube' formation. The complexity and diameters of the 'tubes' in cells treated with 10 ng/ml VEGF-A, 10 ng/ml IL-8 and 10% huLCF, however, was profoundly greater. As with cell proliferation, inclusion of 20 μM SU5416 with the VEGF-A-, IL-8- and huLCF-treated cells dramatically blunted the formation of these structures. To evaluate these observations quantitatively, the average diameters of the 'tubes' that extended between the HMEC-1 clusters were measured (Fig. 7). In comparison to unsupplemented HMEC-1 cells (20 ± 6 μm; n = 4), the 'tube' diameters in cells treated with 10 ng/ml VEGF-A (139 ± 28 μm; n = 4), 10 ng/ml IL-8 (132 ± 21 μm; n = 4) and 10% huLCF (153 ± 23 μm; n = 4) were all significantly increased. Concurrent treatment with 20 μM SU5416 blocked any significant increase in 'tube' diameter growth over control levels. Again, VEGFR signaling accounted for much of the 'tube' development that was induced by factors present within ADPKD liver cyst fluids.

Discussion

ADPKD liver cysts emerge initially as outpockets of cholangiocytes, the epithelial cells that line the intrahepatic bile ducts. As these outpockets continue to grow, they detach from the originating bile duct to become autono-

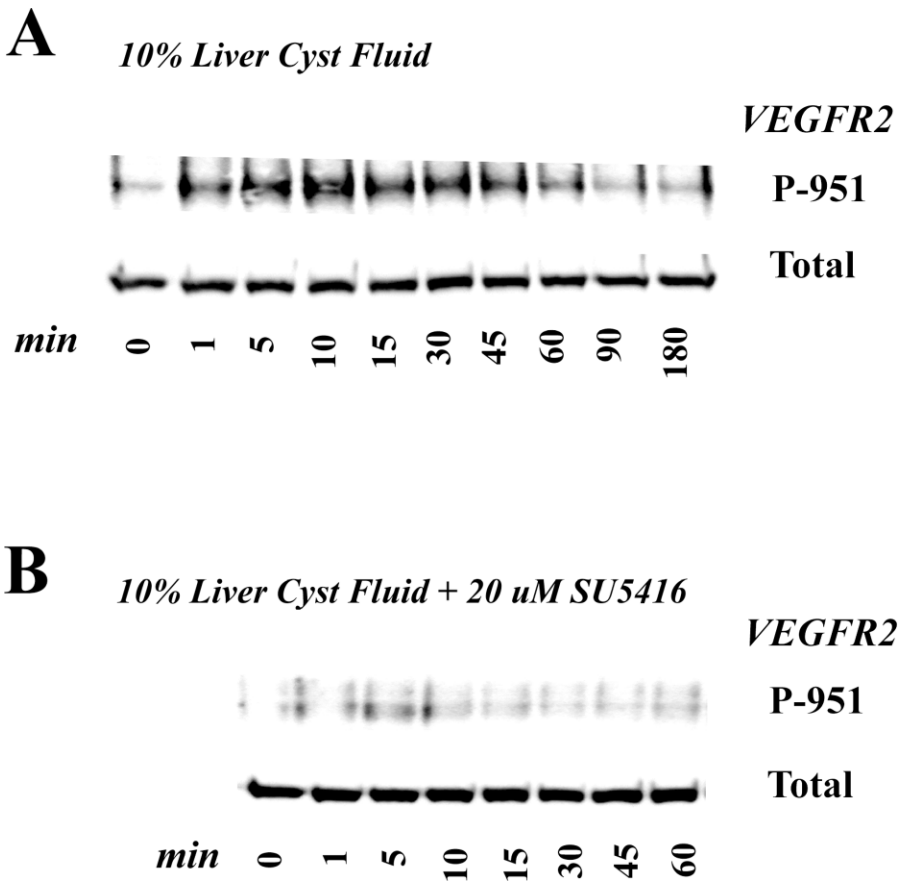

Figure 4. Liver cyst fluid induces phosphorylation of VEGFR2. Incubation of HMEC-1 cells with 10% human liver cyst fluid (huLCF) induces a transient phosphorylation of VEGFR2. (A) Western blot analysis found an increase in VEGFR2 phosphorylation on serine 951 (P-951) after only 1 min of treatment. This effect remained robust for 45 min. After 90 min, VEGFR2 phosphorylation returned to control levels. (B) Pre-treatment with 20 μM SU5416, a VEGF receptor tyrosine kinase inhibitor, markedly inhibited the huLCF-induced increase in VEGFR2 phosphorylation.

mous, enclosed cysts that are lined by 'cystic' cholangiocytes. To meet their metabolic requirements, it is anticipated that the cells within the liver cyst walls would signal for angiogenesis and vascularization of the liver cyst wall. The present studies sought to demonstrate and characterize the presence of the vasculature within pkd2(WS25/-) mouse and human ADPKD liver cyst walls. Subsequently, studies were performed to determine if factors that are secreted by liver cyst-lining epithelial cells, including VEGFR2 and CXCR2 agonists, are capable of inducing proliferation and angiogenic development of endothelial cells.

Vascular Modifications Impact Growth Of Human Liver Cyst Walls. Three published studies support the premise that the liver cyst walls are vascularized and that vascularization is essential for supporting the growth and persistence of liver cysts. First, hepatic artery embolization in human ADPKD patients with significant liver cyst involvement had a 30% decrease in liver cyst volumes 18 to 37 months after therapy (21). Second, a retrospective study of ADPKD patients who received a kidney transplant and received rapamycin in their immunosuppression regimen measured a 12% decrease in the patient's polycystic liver volumes (22). This is compared to a 14% increase in ADPKD patients whose immunosuppression did not include rapamycin. Importantly, rapamycin can inhibit VEGF signaling, VEGF synthesis and angiogenesis (23). Third, long-term treatment of pkd2(WS25/-) mice with SU5416, an inhibitor of VEGF signaling, dramatically impeded liver cyst growth (7). While the effect on the cyst wall vasculature was not specifically accessed, SU5416 has been shown in other studies to have a profound inhibitory effect on endothelial cell development and angiogenesis.

These studies strongly implicated the vasculature as playing an essential role in liver cyst viability and highlighted the need to characterize the vascular system within liver cyst walls. Using complimentary microscopy techniques, the present studies demonstrated that the liver cyst walls in pkd2(WS25/-) mice not only have a substantial vascular network but that the vasculature resides, on average, within 25 μm of the cyst-lining epithelium (Figs. 1, 2 and 3). This close apposition and high density should enable efficient nutrient and waste exchange with the cyst-lining epithelial cells and is consistent with the 'normal' morphology observed in mouse liver cyst epithelial cells (24).

In contrast, human ADPKD liver cyst walls had comparatively low vascular densities and large vessel-to-

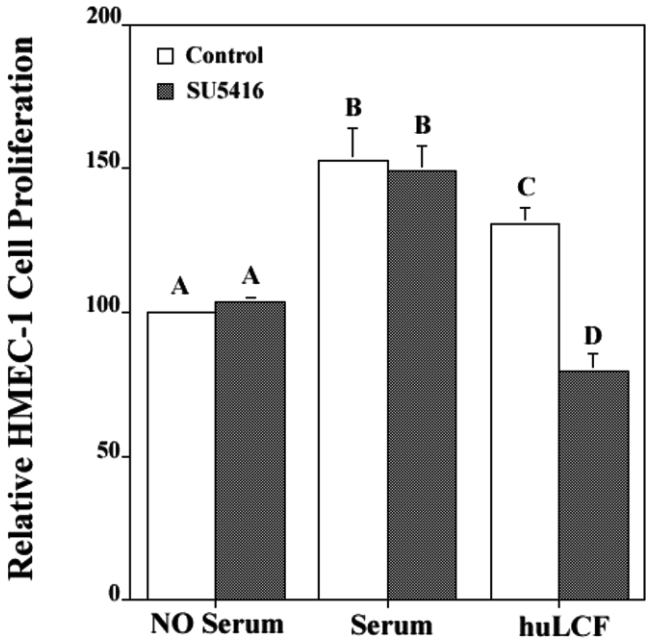

Figure 5. Proliferation of HMEC-1 cells is inhibited by SU5416. HMEC-1 cells (open bars) incubated with 10% human liver cyst fluid (huLCF) showed a significant proliferative response (131 ± 6; n = 12) compared to cells in unsupplemented media (NO Serum: 100 ± 0; n = 3) and in 10% FBS (Serum: 153 ± 11; n = 3). Pre-treatment with 20 μM SU5416 (closed bars) had no discernible effect on the proliferative rates in unsupplemented cells (103 ± 2; n = 3) or cells incubated with 10% FBS (149 ± 9; n = 3). SU5416 did, however, markedly inhibit the proliferative response to 10% huLCF (80 ± 6; n = 12).

epithelium distances (Fig. 3). It should be reiterated that the human liver cyst wall samples were taken during fenestration procedures and were restricted to free walls that had grown out from the body of the liver. It remains unclear how the vasculature is configured in the regions of cyst wall nearer the body of the liver. For the free liver cyst wall, the low degree of vascularization should diminish the oxygen delivery to the human liver cyst wall epithelium and may contribute to the 'ischemic' morphology observed in human liver cyst wall epithelial cells (6). A consistent response of many cell types to ischemia or hypoxia is the induction and synthesis of factors that induce angiogenesis. Not surprisingly, known angiogenic factors, such as VEGF-A and IL-8, are consistently present at significant concentrations in the fluid recovered from human liver cysts (6). It is intriguing that liver cyst fluids from pkd2(WS25/-) mice, which do not display an 'ischemic' phenotype (24), have a similar profile of cytokines and growth factors (6–8). This would suggest that ischemia/hypoxia is not the only parameter responsible for inducing the expression of these factors. Functional alterations in polycystin-1 and polycystin-2, the proteins encoded for by the PKD1 and PKD2 genes, may themselves contribute to the expression of VEGF-A. For example, polycystin-1 complexes with and downregulates the activity of mTOR (25). Thus, mutated polycystin-1 may liberate and increase mTOR activity which, in turn, is capable of elevating VEGF-A expression. Regardless of the stimulus, the presence of pro-angiogenic factors would likely have potent effects in moderating endothelial cell behavior.

VEGF-A and IL-8 Are Positioned to Drive Angiogenesis in Liver Cyst Walls. VEGF-A, IL-8 (humans) and KC (mice) are consistently found in high concentrations in the liver cyst fluids (6–8). The presence of these factors in liver cyst fluids likely reflects the release of these factors across the apical membrane of the cyst-lining epithelium. In order for these factors to interact with the vascular endothelium embedded within the liver cyst wall, they would need to either cross the epithelial layer or be similarly secreted across the basolateral membrane of the cyst-lining epithelium. Electron microscopy of human and mouse liver cyst epithelia shows the presence of intact tight junctions, though regions of detached cell-cell interactions are observed in some human liver cyst walls (6, 24). The transepithelial resistance across cultured mouse liver cyst epithelial monolayers is routinely in excess of 1,000 $\Omega \cdot cm^2$ (24). These observations suggest there would be minimal transepithelial migration of the factors present in the lumenal fluid. However, apical and basal media taken from high resistance monolayers of pkd2(WS25/-) mouse liver cyst epithelial cells have a qualitatively similar profile of cytokines and growth factors in both compartments (7, 8, 24). Among these factors, VEGF-A and KC (murine IL-8 analog) were present in higher concentrations in the basal compartment. This finding indicates that cyst-lining epithlelial cells can secrete VEGFR2 and CXCR2 agonists across their basolateral membrane. If this secretion occurs in native human liver cyst epithelial cells, VEGF-A and IL-8 would be positioned to drive angiogenesis and direct the vascularization of the liver cyst wall. Receptors for VEGF and IL-8 are widely expressed in endothelial cells. Further, VEGFR1 and VEGFR2 are expressed on both arteries and veins that reside within ADPKD liver cyst walls (12).

VEGF-A and IL-8 Act Cooperatively Through VEGFR2. VEGF-A exerts its biological effects on vascular endothelial cells through high-affinity binding to two tyrosine kinase receptors, VEGFR1 (a.k.a. Flt-1) and VEGFR2 (a.k.a. Kdr, Flk-1). Tyrosine phosphorylation of VEGFR2 has been directly associated with receptor activation and subsequent increases in vascular permeability, cell migration and cell proliferation (26). IL-8 signaling occurs through specific G-protein coupled receptors (GPCR), CXCR1 and CXCR2. While both VEGF-A and IL-8 have been individually appreciated for their pro-angiogenic properties, VEGF-A and IL-8 can work cooperatively (19, 27). IL-8-activated CXCR2 can transduce its signal, in part, by transactivating other receptor-signaling systems. In non-small cell cancer cell lines, IL-8 transactivates EGF receptors, a tyrosine kinase receptor, to induce cell proliferation (27). Likewise, IL-8 stimulation of cultured endothelial cells results in transactivation of VEGFR2 (19). In these cells, IL-8-bound CXCR2 complexes with VEGFR2 and promotes tyrosine phosphoryla-

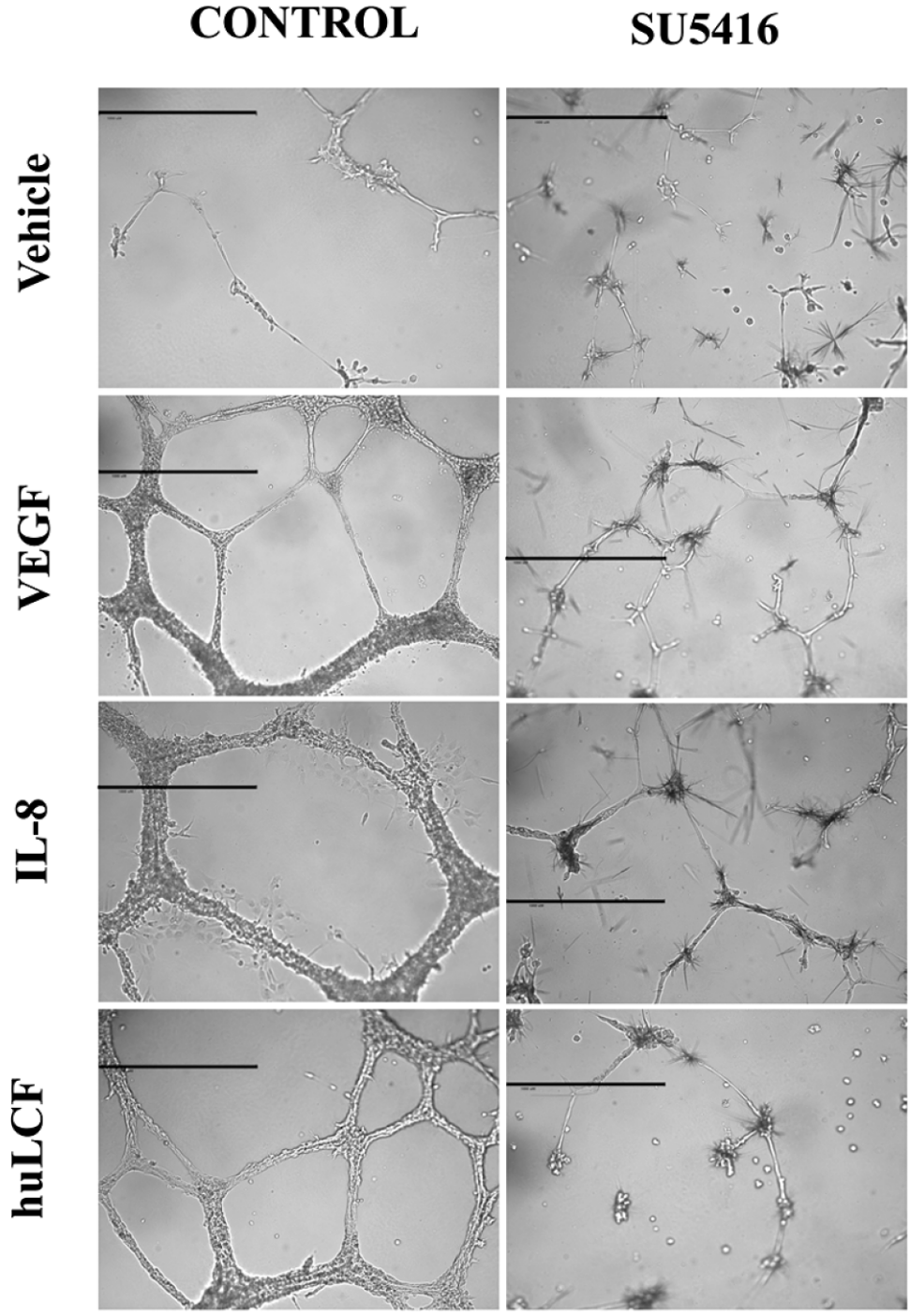

Figure 6. VEGF-A, IL-8 and huLCF induce development of HMEC-1 cells. The panels in the left hand column (control) show HMEC-1 cells seeded and cultured for 24 hr in GF-reduced Matrigel after they received vehicle, 10 ng/ml VEGF-A, 10 ng/ml IL-8 or media containing 10% huLCF. Vehicle-treated cells showed only modest levels of cell migration, proliferation or 'tube' formation. In contrast, cells treated with VEGF-A, IL-8 and huLCF each showed remarkable reorganization to form a series of broad, interconnected 'tubes.' The panels in the right hand column (SU5416) show that 20 μM SU5416 profoundly blocked the developmental response to VEGF-A, IL-8 and huLCF.

tion of VEGFR2 in an src-dependent manner. This VEGFR2 transactivation is required for the IL-8-dependent moderation of endothelial cell permeability. In support of this, initial studies (data not shown) showed that VEGF-A and IL-8 increased the rate of HMEC-1 cell proliferation and that both the VEGF-A and IL-8 proliferative responses were inhibited by pre-treatment with 20 μM SU5416. This confirmed that the IL-8 proliferative effects in endothelial cells required transactivation of VEGFR2. Given the consistent coincident expression of VEGF-A and IL-8 in liver cyst fluids and the convergence of their signaling mechanisms through VEGFR2, it is attractive to speculate

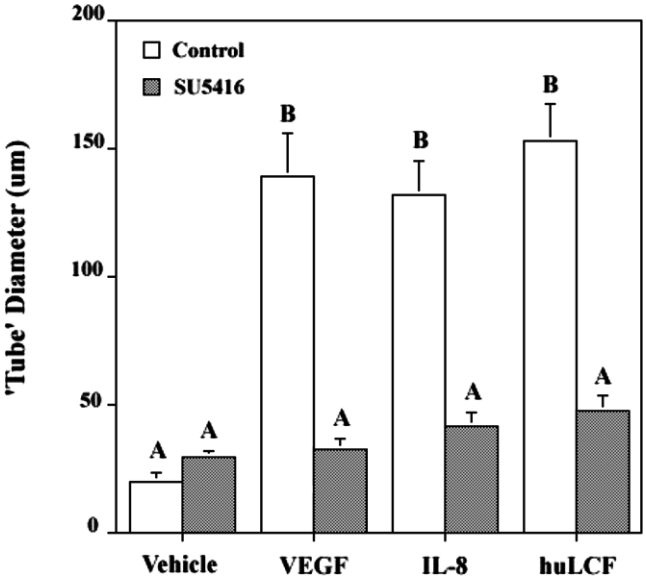

Figure 7. VEGF-A, IL-8 and huLCF promote increased 'tube' widths in HMEC-1 cells. In HMEC-1 cells (open bars), the 'tube' width that developed after 24 hr was significantly greater in cultures that included 10 ng/ml VEGF-A (139 ± 28 μm; n = 4), 10 ng/ml IL-8 (132 ± 21 μm; n = 4) and 10% huLCF (153 ± 23 μm; n = 4) compared to cells in unsupplemented media (vehicle: 20 ± 6 μm; n = 4). Co-treatment with 20 μM SU5416 (closed bars) blocked the increase in 'tube' diameters induced by VEGF-A (33 ± 6 μm; n = 4), IL-8 (42 ± 9 μm; n = 4) and huLCF (48 ± 11 μm; n = 4) and were not significantly different than SU5416-treated vehicle cells (30 ± 4 μm; n = 4).

these two factors combine to induce a robust and prolonged activation of VEGFR2 and that activated VEGFR2 drives angiogenesis in the liver cyst wall.

The present studies provide an initial step in testing and validating this speculation. HuLCFs were used to approximate the composite of factors released across the basolateral membrane of liver cyst epithelial cells. Treatment of human HMEC-1 endothelial cells with 10% huLCF resulted in increased VEGFR2 phosphorylation, and indicator of receptor activation (Fig. 4). Furthermore, this increased phosphorylation was inhibited by pre-treatment with 20 μM SU5416. Likewise, treatment of HMEC-1 cells with 10% huLCF induced increased rates of cell proliferation (Fig. 5) and development of multi-cellular 'vasculature-like' structures (Fig. 6). Again, these phenotypic effects were blocked by inhibiting VEGFR2 activation. While other factors are also secreted by liver cyst epithelia, the marked sensitivity of both the proliferative and developmental responses to VEGFR2 inhibition suggest VEGFR2 signaling is the key effector pathway. More broadly, the present studies support the importance of future *in vivo* studies to determine if the inhibition of liver cyst growth by SU5416 is due to alterations in endothelial cell maintenance and viability.

The tissue preparation, imaging and morphometry in the electron microscopy studies were expertly performed by Rolf Dahl. Dr. Sean Colgan (University of Colorado, Denver) kindly provided the HMEC-1 cells and contributed significantly to the refinement of the 'tube formation' assay. The pkd2(WS25/-) breeding pairs were graciously provided by Dr. Stefan Somlo (Yale University).

1. Bae KT, Zhu F, Chapman AB, Torres VE, Grantham JJ, Guay-Woodford LM, Baumgarten DA, King BF, Wetzel LH, Kenney PJ, Brummer ME, Bennett WM, Klahr S, Meyers CM, Zhang X, Thompson PA, Miller JP. MRI evaluation of hepatic cysts in early ADPKD. Clin J Am Soc Nephrol 1:64–69, 2006.
2. Wall WJ. Liver transplantation for polycystic liver disease. New Eng J Med 356:1560, 2007.
3. Doctor RB, Nash R, Nichols MT, Everson GT. Fibrocystic diseases of the liver. In: Boyer TD, Wright TL and Manns MP, Eds. Hepatology: A Textbook of Liver Disease (5th ed.).. Philadelphia, PA: Saunders-Elsevier, pp 1329–1354, 2006.
4. Harris PC, Bae KT, Rossetti S, Torres VE, Grantham JJ, Chapman AB, Guay-Woodford LM, King BF, Wetzel LH, Baumgarten DA, Kenney PJ, Consugar M, Klahr S, Bennett WM, Meyers CM, Zhang QJ, Thompson PA, Zhu F, Miller JP. Cyst number but not the rate of cystic growth is associated with the mutated gene in ADPKD. J Am Soc Nephrol 17:3013–3019, 2006.
5. Fain PR, McFann KK, Taylor MRG, Tison M, Johnson AM, Reed B, Schrier RW. Modifier genes play a significant role in the phenotypic expression of PKD1. Kidney Int 67:1256–1267, 2005.
6. Nichols MT, Gidey E, Matzakos T, Dahl R, Stiegmann G, Shah RJ, Grantham JJ, Fitz JG, Doctor RB. Secretion of cytokines and growth factors into ADPKD liver cyst fluid. Hepatology 40:836–846, 2004.
7. Amura CR, Brodsky KF, Groff R, Gattone V, Voelkel NF, Doctor RB. VEGF signaling promotes ADPKD liver cyst growth in pkd2(WS25/-) mice. Am J Physiol 293:C419–C428, 2007.
8. Amura CR, Brodsky KF, Gitomer B, McFann K, Lazennec G, Nichols MT, Jani A, Schrier RW, Doctor RB. CXCR2 agonists in ADPKD liver cyst fluids promote cell proliferation. Am J Physiol 294:C786–C796, 2008.
9. Lee J, Horuk R, Rice G, Bennett G, Camerato T, Wood W. Characterization of two high affinity human IL-8 receptors. J Biol Chem 267:16283–16287, 1992.
10. Mustonen T, Alitalo K. Endothelial receptor tyrosine kinases involved in angiogenesis. J Cell Biol 129:895–898, 1995.
11. Wu G, D'Agati V, Cai Y, Markowitz GS, Park JH, Reynolds DM, Maeda Y, Le TC, Hou HJ, Kuchrlapati R, Edelmann W, Somlo S. Somatic inactivation of Pkd2 results polycystic kidney disease. Cell 93: 177–188, 1998.
12. Fabris L, Cadamuro M, Fiorotto R, Roskams T, Spirli C, Melero S, Sonzogni A, Joplin RE, Okolicsanyi L, Strazzabosco M. Effects of angiogenic factor overexpression by human and rodent cholangiocytes in polycystic liver diseases. Hepatology 43:1001–1012, 2006.
13. Mohler W, Millard AC, Campagnola PJ. Second harmonic generation imaging of endogenous structural proteins. Methods 29:97–109, 2003.
14. Doctor RB, Dahl RH, Salter KD, Fitz JG. Reorganization of cholangiocyte membrane domains represents an early event in rat liver ischemia. Hepatology 29:1364–1374, 1999.
15. Ades EW, Candal FJ, Swerlick RA, George VG, Summers S, Bosse DC, Lawley TJ. HMEC-1: establishment of an immortalized human microvascular endothelial cell line. J Invest Derm 99:683–690, 1992.
16. Doctor RB, Bennett V, Mandel LJ. Degradation of spectrin and ankyrin in the ischemic rat kidney. Am J Physiol 264:C1003–C1013, 1993.
17. Madri JA, Pratt BM, Tucker AM. Phenotypic modulation of endothelial cells by TGFb depends on the composition and organization of the extracellular matrix. J Cell Biol 106:1375–1384, 1988.
18. Kong T, Westerman KA, Faigle M, Eltzschig HK, Colgan SP. HIF-dependent induction of adenosine A2B receptor in hypoxia. FASEB J 20:2242–2250, 2006.
19. Petreaca ML, Yao M, Liu Y, DeFea K, Martins-Green M. Trans-

activation of VEGFR2 by IL-8 is required for IL-8/CXCL8-induced endothelial permeability. Mol Biol Cell 18:5014–5023, 2007.

20. Fong TAT, Shawver LK, Sun L, Tang C, App H, Powell TJ, Kim YH, Schreck R, Wang X, Risau W, Ullrich A, Hirth KP, McMahon G. SU5416 is a potent and selective inhibitor of the VEGF receptor (Flk-1/KDR) that inhibits tyrosine kinase catalysis, tumor vascularization and growth of multiple tumor types. Cancer Res 59:99–106, 1999.
21. Takei R, Ubara Y, Hoshino J, Higa Y, Suwabe T, Sogawa Y, Nomura H, Nakanishi S, Sawa N, Katori H, Takemoto F, Hara S, Takaichi K. Percutaneous transcatheter hepatic artery embolization for liver cysts in ADPKD. Am J Kid Dis 49:744–752, 2007.
22. Qian F, Du H, King BF, Kumar S, Dean PG, Cosio FG, Torres VE. Sirolimus reduces polycystic liver volume in ADPKD patients. J Am Soc Nephrol 19:631–638, 2008.
23. Guba M, von Breitenbuch P, Steinbauer M, Koehl G, Flegel S, Hornung M, Bruns CJ, Zuelke C, Farkas S, Anthuber M, Jauch KW, Geissler EK. Rapamycin inhibits primary and metastatic tumor growth by antiangiogenesis: involvement of vascular endothelial growth factor. Nature Med 8:128–135, 2002.
24. Doctor RB, Johnson S, Brodsky KS, Amura CR, Gattone V, Fitz JG. Regulated ion secretion in liver cyst epithelia. Biochim Biophys Acta 1772:345–354, 2007.
25. Shillingford JM, Murcia NS, Larson CH, Low SH, Hedgepeth R, Brown N, Flask CA, Novick AC, Goldfarb DA, Kramer-Zucker A, Walz G, Piontek KB, Germino GG, Weinmbs T. The mTOR pathway is regulated by polycystin-1, and its inhibition reverses renal cystogenesis in polycystic kidney disease. Proc Natl Acad Sci U S A 103: 5466–5471, 2006.
26. Holmes K, Roberts OL, Thomas AM, Cross MJ. VEGFR2: Structure, function, intracellular signaling and therapeutic inhibition. Cellular Signal 19:2003–2012, 2007.
27. Luppi F, Longo AM, deBoer WI, Rabe KF, Hiemstra PS. IL-8 stimulates cell proliferation in non-small lung cancer through EGFR transactivation. Lung Canc 56:25–33, 2007.